

# Modelling Carbon Radio Recombination Line observation towards the Ultra-Compact H II region W48A

S. Jeyakumar<sup>1,3\*</sup> and D. Anish Roshi<sup>2†</sup>

<sup>1</sup> *Departamento de Astronomía, Universidad de Guanajuato, AP 144, Guanajuato CP 36000, Mexico*

<sup>2</sup> *National Radio Astronomy Observatory‡, Charlottesville, VA 22903-4608, USA*

<sup>3</sup> *Raman Research Institute, C. V. Raman Avenue, Sadashivanagar, Bangalore - 560 080, India*

## ABSTRACT

We model Carbon Recombination Line (CRL) emission from the Photo Dissociation Region (PDR) surrounding the Ultra-Compact (UC) H II region W48A. Our modelling shows that the inner regions ( $A_V \sim 1$ ) of the C II layer in the PDR contribute significantly to the CRL emission. The dependence of line ratios of CRL emission with the density of the PDR and the far ultra-violet (FUV) radiation incident on the region is explored over a large range of these parameters that are typical for the environments of UCH II regions. We find that by observing a suitable set of CRLs it is possible to constrain the density of the PDR. If the neutral density in the PDR is high ( $\gtrsim 10^7 \text{ cm}^{-3}$ ) CRL emission is bright at high frequencies ( $\gtrsim 20 \text{ GHz}$ ), and absorption lines from such regions can be detected at low frequencies ( $\lesssim 10 \text{ GHz}$ ). Modelling CRL observations towards W48A shows that the UCH II region is embedded in a molecular cloud of density of about  $4 \times 10^7 \text{ cm}^{-3}$ .

**Key words:** Atomic processes – ISM: clouds – ISM:HII regions – Radio lines: ISM

## 1 INTRODUCTION

HII regions with size less than about 0.1 pc are called Ultra Compact HII regions (UCH II regions). Their radio continuum emission is optically thick at frequencies below a few GHz indicating emission measures  $\gtrsim 10^7 \text{ pc cm}^{-6}$  and electron densities  $\gtrsim 10^4 \text{ cm}^{-3}$  (cf. Wood & Churchwell 1989a; Kurtz et al. 1994; Garay & Lizano 1999). Molecular line observations reveal that UCH II regions are embedded in dense molecular clouds (e.g. Kim & Koo 2003). Line emission from many high density tracer molecules, such as  $\text{NH}_3$ , and CS, is detected towards some of the UCH II regions (cf. Churchwell et al. 1990; Garay & Lizano 1999; Kim & Koo 2003). The UCH II regions are bright at far-infrared wavelengths and modelling this emission suggests hot dust envelopes surrounding newly formed stars (Churchwell 1993; Kurtz et al. 1994). Some of these sources also show evidence for internal density and velocity gradients within the ionised region (Sewifo et al. 2008; Keto et al. 2008; Phillips 2007). These observations imply that UCH II regions are early evolutionary stages of massive stars, and embedded in dense massive molecular clouds with high optical extinctions (cf. Churchwell 2002).

The age of UCH II regions estimated from the observed num-

ber of such H II regions in the Galaxy and the galactic star formation rate is  $\sim 10^5$  years. This age is found to be longer than the time scale of expansion of the ionised gas to a size of about 0.1 pc (dynamical age; a few times  $10^3$  years) at its sound speed (cf. Wood & Churchwell 1989b). Many models have been proposed to resolve this inconsistency in age or otherwise called the *age paradox* (cf. Franco et al. 2007; Garay & Lizano 1999, and references therein). The proposed models include, (a) confinement of ionized gas due to thermal or turbulent pressure of surrounding material, (b) confinement by ram pressure of infalling material or bow shocks (c) champagne flows, (d) disk evaporation, (e) mass loaded stellar wind. Recently Peters et al. (2010) proposed that ‘flickering’ of the size of the ionized regions around massive stars due to shielding by dense filaments in accretion flow makes the size of the H II region independent of the age of the star. Many of these models need dense external medium surrounding the ionised gas (e.g. de Pree et al. 1995). Indeed, observations of molecular and carbon recombination lines (CRL) have also shown the presence of high-density ( $> 10^5 \text{ cm}^{-3}$ ) molecular material in the vicinity of UCH II regions (Roshi et al. 2005b).

The high-density molecular material surrounding UCH II regions can be heated by the FUV radiation from the embedded massive stars, establishing a Photo Dissociation Region (PDR) (cf. Tielens & Hollenbach 1985). The PDR in the vicinity of the H II region forms a thin layer, mostly consisting of ionised carbon (CII) and neutral hydrogen (HI). The physical conditions in this layer can be inferred by observing [CII], [OI] and ro-vibrational  $\text{H}_2$  emission lines (cf. Hollenbach & Tielens 1997), which are all in

\* Email: sjk@astro.ugto.mx

† Email: aroshi@nrao.edu

‡ The National Radio Astronomy Observatory is a facility of the National Science Foundation operated under cooperative agreement by Associated Universities, Inc.

the infra-red band. The recombination of an electron with a carbon ion at high quantum numbers,  $n \geq 40$ , and subsequent cascade produces CRLs in the radio frequencies. Observations of these CRLs can also be used to infer the physical conditions of the PDR (e.g. Roelfsema & Goss 1992; Natta et al. 1994; Roshi et al. 2005a). Amplification of the CRL by the background continuum emission makes it possible to detect these lines easily with the existing radio telescopes (cf. Dupree & Goldberg 1970). Such stimulated CRL emission is observed towards many regions of ionised carbon in the Galaxy (e.g. Natta et al. 1994; Wyrowski et al. 1997; Roshi et al. 2002, and references therein). Roshi et al. (2005a) also detected stimulated CRL emission near 8.5 GHz from PDRs associated with a large number of UCH II regions.

Attempts have been made earlier to infer the physical conditions in the PDR using CRL emission with the help of detailed PDR models (Gomez et al. 1998). Natta et al. (1994) studied the line intensity ratio of C91 $\alpha$  (near 8.6 GHz) and C66 $\alpha$  (near 24 GHz) transitions using a limited set of homogeneous PDR models with densities in the range  $10^4$  and  $10^7$  cm $^{-3}$  and incident FUV field between  $10^3$  and  $10^6$   $G_0$ , where  $G_0$  is the standard interstellar FUV field ( $1.6 \times 10^{-3}$  ergs cm $^{-2}$  s $^{-1}$ ) of Habing (1968).

However, based on the observational studies of the UCH II regions and their environment, the ranges of PDR and UCH II region properties are expected to be larger. The densities of the molecular material near UCH II regions inferred from observations of high density tracer molecule, NH $_3$ , are in the range of a few times  $10^4$  to  $10^8$  cm $^{-3}$  (cf. Garay & Lizano 1999). The expected FUV field at the surface of UCH II regions due to the embedded O4 to B0 type stars ranges from  $10^4$  to greater than  $10^7$   $G_0$  (Wood & Churchwell 1989b).

Therefore, in this paper, we examine a complete set of PDR models, spanning a large range of densities and incident radiation field which are required to model the CRL emission observed towards UCH II regions. The details of modelling are discussed in Section 2. In Section 3, we show that a multitude of recombination transitions from PDRs near UCH II regions can be used to constrain the physical conditions of this layer. We apply our model to interpret the observed CRL emission towards W48A in Section 4.

## 2 PDR SURROUNDING AN UCH II REGION

PDR is created at the interface between an UCH II region and the associated molecular cloud. During the early phases of the evolution of H II regions, the existence of the PDR layer depends on the relative speed between the ionisation and the dissociation fronts (Bertoldi & Draine 1996). However, UCH II regions can attain pressure equilibrium within the dense molecular cores (Kurtz et al. 2001), and the high pressure cores can stop the expansion at a time scale of about  $3 \times 10^4$  yr (Franco et al. 2000). Arthur et al. (2004) noted that the dust in the ionised region can stall the expansion even earlier. This time scale is a factor of about 10 smaller than the age inferred from the observed number of UCH II regions (Wood & Churchwell 1989b) suggesting that the H II regions may be pressure confined for a long time. CRL observations towards UCH II regions also indicate that these H II regions may be pressure confined (Roshi et al. 2005a).

The PDRs can attain steady state if the age of these regions is much larger than the time scales of cooling and molecular processes. The cooling time scale is of the order of  $4 \times (T/1000)^{-7/2}$  yr, which is much smaller than the evolutionary time scales (Hollenbach & Natta 1995) for the typical tempera-

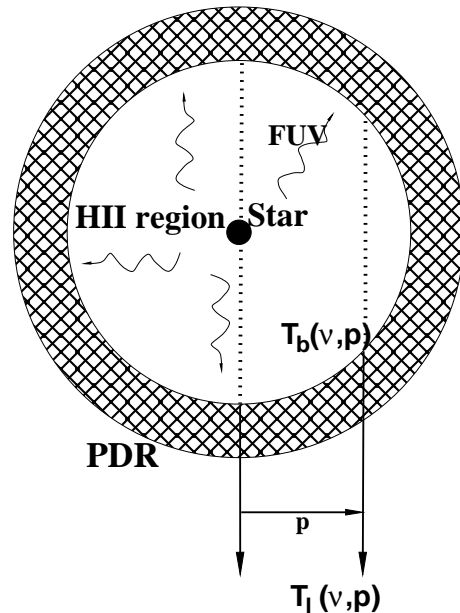


**Figure 1.** A schematic of the geometry used for the CRL intensity calculations (not to scale). The PDR layer, shown as shaded region, surrounds the UCH II region. The FUV radiation from the central star in the H II region produces the PDR layer. The background continuum  $T_b(\nu, p)$  for each ray with impact parameter,  $p$ , is calculated along the dotted lines.  $T_l(\nu, p)$  is the calculated line brightness temperature corresponding to this ray.

ture of a few 10s to  $\sim 1000$  K in the PDR. Of the chemical processes, the slower hydrogen formation time scale,  $\tau_{H_2}$ , is about  $5 \times 10^8/n$  yr, where  $n$  is the hydrogen gas density in cm $^{-3}$  (Goldshmidt & Sternberg 1995). For densities  $\geq 10^5$  cm $^{-3}$ ,  $\tau_{H_2}$  is  $< 5000$  yr, which is shorter than the expected age or the time scale for pressure equilibrium. This suggests that the PDR surrounding the UCH II regions can attain steady state in a relatively short time scale for high ambient gas densities.

For an expanding UCH II region the PDR properties evolve with time (Franco et al. 1990; Roger & Dewdney 1992). In this case, the thermal equilibrium is achieved faster than the dynamical time scales (Hollenbach & Natta 1995), but the effect of time dependent chemistry might be important. In this paper, we consider the case where the PDR is in a steady state.

### 2.1 Model for Carbon recombination lines

We consider a spherical UCH II region of radius,  $R_{HII}$ , placed inside a molecular medium of density  $n$ , for modelling. The ionising star is assumed to be at the centre of the UCH II region and is stationary with respect to the molecular cloud. The molecular material is heated by the FUV radiation from the embedded star, establishing a PDR layer as shown schematically in Fig. 1. The FUV field incident on the surface of the molecular medium,  $G$ , is specified in units of the mean interstellar radiation field  $G_0$  (cf. Le Petit et al. 2006). For a given FUV field and a molecular density, the PDR models solve the energy balance and the chemical network simultaneously. This solution provides the equilibrium gas temperature,  $T_e$ , and the density of ionised carbon,  $n_{CII}$ , as well as that of the electron,  $n_e$ , as a function of depth into the molecular medium measured from the surface of incidence of FUV radiation (cf. Le Bourlot et al. 1993). For the present work, these results for the PDR are obtained using the Meudon-PDR code (ver-

sion 13XI03) developed by Le Bourlot et al. (1993) where a 1 D, semi-infinite plane parallel slab of gas is heated from one side by the FUV field. The standard values of all other parameters of this model, such as the heating and cooling processes, can be obtained from the above reference. We used the standard chemical network available with this code (file named Drcos.chi) which uses a total of 69 chemical species and 539 chemical reactions.

For the calculation of CII level populations, we approximate the PDR layer into  $N_{slab}$  slabs each with a constant  $T_e$ ,  $n_e$  and  $n_{CII}$ . The level populations of the CII levels are calculated for each slab. The effects of deviation of the level populations from LTE on the line emission are characterised by the factors,  $b_n$  and  $\beta_n$  (cf. Dupree & Goldberg 1970). These factors are calculated using the code originally developed by Salem & Brocklehurst (1979) and later modified by Walmsley & Watson (1982) and Payne et al. (1994). The excitation of carbon levels are affected by the background radio continuum radiation and local gas collisions. Since the free-free optical depth of the PDR layer for the frequencies of interest here is negligible, all the slabs receive the same background continuum intensity. The temperature of the background radiation incident at the surface of the PDR layer, at any given frequency is determined using the electron temperature and emission measure of the ionised gas in the spherical UCH II region (Mezger & Henderson 1967).

For estimating the CRL intensities, we substituted the radial dependence of the physical quantities of the spherical PDR shell by the 1 D results obtained as described above. The emergent intensity is calculated for many rays ( $\sim 200$ ). Each ray is identified with an impact parameter,  $p$  (see Fig. 1), which is measured from the centre of the sphere and has values in the range 0 to  $R_{HII}$ . The background continuum for each ray is calculated through the chord shown as dashed lines in Fig 1.

Following Shaver (1975) the line radiation temperature for a ray with impact parameter,  $p$ , is given by,

$$T_l(\nu, p) = T_{l+c}(\nu, p) - T_c(\nu, p); \quad (1)$$

where

$$T_{l+c}(\nu, p) = T_b(\nu, p) \exp(-\tau_l^T - \tau_c^T) + \int_0^{\tau_l^T + \tau_c^T} T_{ex}(\nu, \tau') \exp(-\tau') d\tau', \quad (2)$$

$$T_c(\nu, p) = T_b(\nu, p) \exp(-\tau_c^T) + \int_0^{\tau_c^T} T_{ex}(\nu, \tau') \exp(-\tau') d\tau'. \quad (3)$$

In the above equations  $\nu$  is the frequency of the transition.  $\tau'$  is the optical depth to a point in the PDR layer measured from the outer boundary.  $\tau^T$  is the total optical depth of the PDR layer. The subscripts  $l$  and  $c$  denote the line and continuum respectively.  $T_b$  and  $T_{ex}$  are the background radio continuum radiation temperature and excitation temperature of the CII levels respectively. The surface averaged line radiation temperature is obtained as

$$T_L(\nu) = \frac{\int_0^{R_{HII}} T_l(\nu, p) 2\pi p dp}{\int_0^{R_{HII}} 2\pi p dp}.$$

### 3 FORMATION OF CRL IN PDR

For understanding the CRL formation in PDR, the contribution to the total CRL emission, of each thin shell within the PDR layer surrounding the UCH II region is studied. The combined PDR and

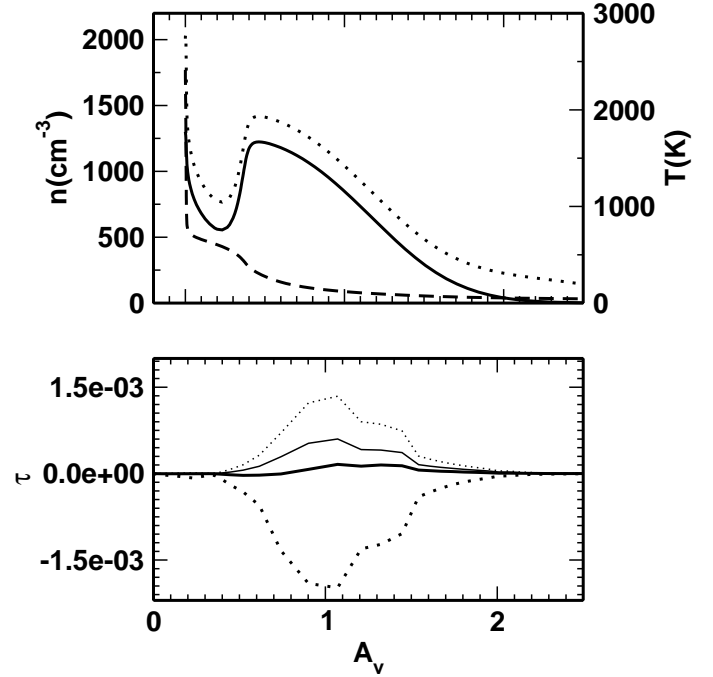


**Figure 2.** In the upper panel, the density of  $C^+$  (solid) and electron (dotted) and the temperature of the gas (dashed) are plotted against the depth into the molecular cloud measured in  $A_V$ . These results are obtained using the PDR model, for a density of  $10^7 \text{ cm}^{-3}$  and an FUV field of  $10^4 G_0$ . In the lower panel, the CRL optical depths are plotted against  $A_V$ , for the same PDR properties shown in the upper panel. The LTE optical depths for  $C53\alpha$  and  $C76\alpha$  are shown by the thin solid and thin dashed lines respectively. Note that the LTE optical depths have positive values for all  $A_V$ . The non-LTE optical depths of these transitions are shown with the thick solid and thick dashed lines respectively. The non-LTE optical depths have been multiplied by a factor of 5 for displaying.

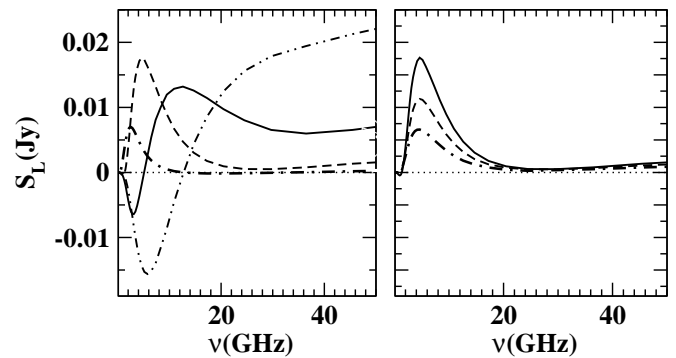


**Figure 3.** The CRL flux density is plotted against frequency for different PDR densities (left) and background FUV flux densities (right). In the left panel, the dot-dot-dashed, continuous, dashed and dot-dashed lines represent line flux density for neutral densities  $10^8$ ,  $10^7$ ,  $10^6$  and  $10^5 \text{ cm}^{-3}$  respectively. The FUV field for these calculations is kept at a constant value of  $10^4 G_0$ . In the right panel, the continuous, dashed and dot-dashed lines represent  $G$  of  $10^4$ ,  $10^5$  and  $10^6 G_0$  respectively. The neutral density used for these calculations is  $10^6 \text{ cm}^{-3}$ .

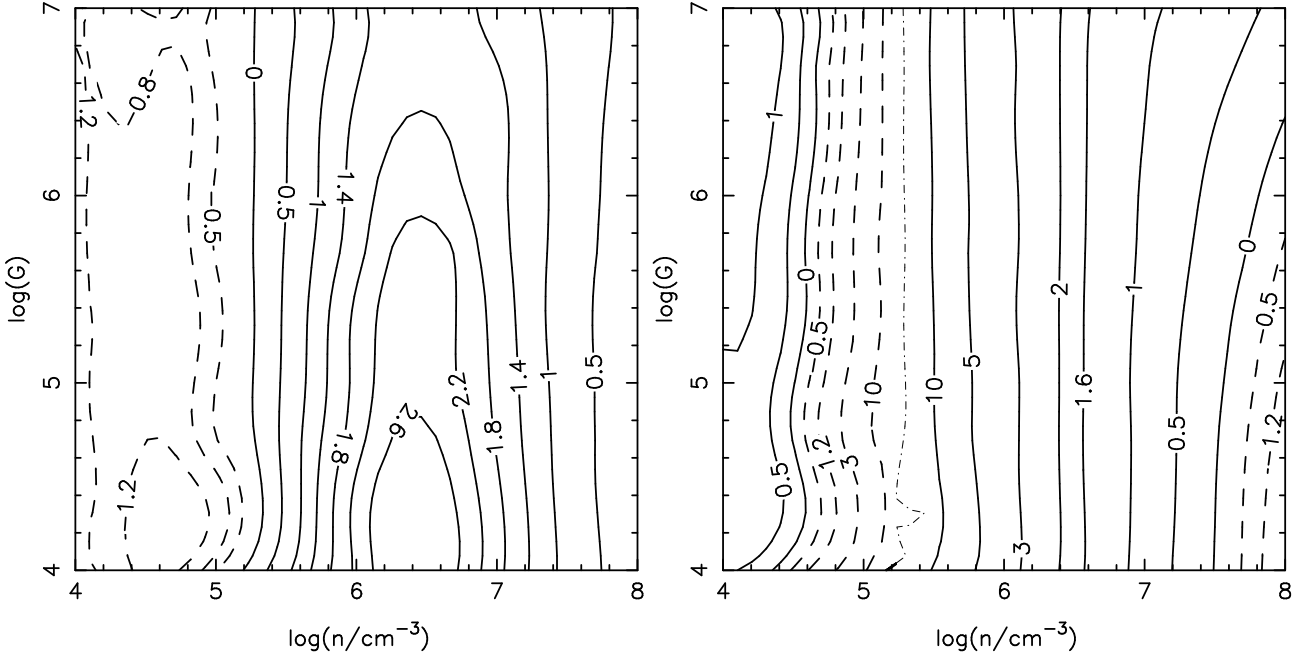


**Figure 4.** The CRL flux density ratios  $C76\alpha/C53\alpha$ (left panel) and  $C92\alpha/C76\alpha$ (right panel) are plotted in the  $\log(n/\text{cm}^{-3})-\log(G)$  plane. The dashed and solid lines show contours of negative and positive ratios respectively. The thin dot-dashed line indicates those ratios where the denominator is zero. The CRL flux densities are obtained by considering a UCH II region with  $EM = 6.4 \times 10^7 \text{ pc cm}^{-6}$ ,  $T_e = 9900 \text{ K}$  and  $R_{\text{HII}} = 0.059 \text{ pc}$ . The negative contours in both panels for densities below  $\sim 10^5 \text{ cm}^{-3}$  are due to the negative values of  $C76\alpha$  (see Fig. 3). In the right panel, the  $C92\alpha$  flux density is negative at very low densities ( $< 10^{4.5} \text{ cm}^{-3}$ ) providing positive line ratio. The negative contours at very high densities ( $> 10^{7.5} \text{ cm}^{-3}$ ) are due to  $C92\alpha$  flux density being negative.

CRL model as described in Section 2 is calculated for the observed parameters of W48A (see Section 4). Using these calculations various characteristics of CRL formation can be understood.

The CRL optical depth as a function of depth into the PDR is obtained by considering a molecular cloud of density  $10^7 \text{ cm}^{-3}$  heated by an FUV flux of  $10^4 G_0$ . The densities of  $C^+$  and electrons and the gas temperature provided by the PDR model for these parameters are plotted as a function of  $A_V$  in Fig. 2 (upper panel). Using these quantities the LTE and non-LTE optical depths of  $C53\alpha$  (45.4764 GHz) and  $C76\alpha$  (14.6973 GHz) are computed, which are also plotted as a function of  $A_V$  in Fig. 2 (lower panel). As seen in Fig. 2 both LTE and non-LTE optical depths have large (absolute) values near  $A_V \sim 1$  for the PDR properties considered for modelling. The CRL optical depth is proportional to  $EM/T_e^{5/2}$  and hence will have large values at those  $A_V$  where this factor is maximum. The non-LTE effect depends on a number of factors such as background radiation field and electron and ion densities. It is expected that the non-LTE optical depth becomes negative for a set of frequencies resulting in partial masing of the recombination line (Shaver 1975). For example, the non-LTE optical depth calculated for the model parameters considered here indicates that the intensity of  $C76\alpha$  is amplified by stimulated emission (see Fig. 2).

From modelling the Spectral Energy Distributions (SEDs) of smaller HII regions (including the Hyper-Compact HII regions) over a wide range in frequency, Keto et al. (2008) infer density gradients, with power-law indices between -1.5 and -2.5. The SEDs of HII regions with such density gradient will be different from those with uniform density, spherical ionized gas considered in the CRL modeling. Typically such SED's have higher radio flux density near frequencies ( $> 10 \text{ GHz}$ ) where the uniform density models become optically thin (e.g. Keto et al. 2008). At frequencies less than about 15 GHz, stimulated emission of CRLs due to background radiation

occurs and hence higher line flux density is expected compared to the uniform density models. Similarly if the lines at these frequencies are in absorption, once again large line flux densities are expected. Therefore the model results presented here are applicable for UCH II regions that do not show evidence of density profiles in their SEDs.

Such density gradients can also be present in the molecular gas in the vicinity of the HII regions. Since the thickness of the layer that contributes to the CRLs is very small, any variation of the physical parameters within this layer is not expected to contribute significantly for the above observed indices. Further, we compared the variation of the LTE optical depths inside a medium with a density gradient with a power-law index of -2.0 (for  $n = 10^7 \text{ cm}^{-3}$ ,  $G = 10^5 G_0$  and  $n = 10^8 \text{ cm}^{-3}$ ,  $G = 10^6 G_0$ ), with those of the appropriate constant density models such that the mean density of the CII layers in both the models are the same. The differences in the variation of the optical depth with distance are negligible between these models. Therefore constant molecular gas density models are a good approximation for modelling the CRLs. However the densities inferred using the CRL emitting PDR layer would imply higher densities at the surface of the HII region for a power-law density medium as compared to a constant density medium.

### 3.1 Dependence of CRL intensity on frequency

The variation of CRL flux density with the frequency of the line transition for different PDR densities ( $10^5, 10^6, 10^7$  and  $10^8 \text{ cm}^{-3}$ ) are shown in Fig. 3 (left panel). An FUV field of  $10^4 G_0$  and UCH II region with parameters described above are used for the flux density calculations. Qualitatively, Fig. 3 (left panel) shows that, for a given FUV field, the maxima of line emission shifts to higher frequencies with increasing density.

The variation of CRL flux density for different line transition with incident FUV field ( $10^4$ ,  $10^5$  and  $10^6 G_0$ ) is shown in Fig. 3 (right panel). A neutral density of  $10^6 \text{ cm}^{-3}$  for the PDR and UCH II region with parameters described above are used for these calculations. The figure shows that the flux density generally decreases with increasing FUV field. This decrease in flux density is because of the general increase in the PDR temperature with the FUV field. The CRL optical depth inversely depends on the PDR temperature ( $T_e^{-5/2}$ ) and hence the flux density decreases with the FUV field.

Examination of the frequency dependence of the CRL flux density (Fig. 3) shows that for densities  $\geq 10^7 \text{ cm}^{-3}$ , it may be possible to detect CRL in absorption at frequencies below  $\sim 10$  GHz. The absorption at low frequencies occurs since the level population of quantum states corresponding to these frequencies approach the LTE value at higher densities. The LTE excitation temperature for these transitions is smaller than the background radiation temperature of the UCH II region.

### 3.2 CRL from an expanding UCHII region

Modeling shows that, for densities typical for PDRs near UCH II regions, it is possible to detect line emission at smaller quantum numbers (ie higher frequencies;  $\geq 20$  GHz or so). This is evident from Fig. 3 for densities  $\geq 10^7 \text{ cm}^{-3}$  where line emission is detectable at frequencies above  $\sim 20$  GHz. The non-LTE optical depth of these lines are positive (see for example Fig. 2) indicating that the line emission is not dominated by stimulated emission. Therefore, for the geometry of the PDR shown in Fig. 1, detecting line emission at frequencies  $\geq 20$  GHz gives an unique opportunity to constrain the expansion speed of the UCH II region. At these frequencies any expansion will produce a double profile for the CRL emission and the separation between the two line components gives a direct measure of the expansion of the UCH II region. Application of this method to the UCH II regions will be discussed further in a forthcoming paper.

### 3.3 Dependence of CRL intensity on PDR parameters

The ranges of PDR parameters over which we present the model results are chosen based on the observational studies of the environments of the H II regions. The densities of the molecular material near UCH II regions inferred from observations of high density tracer molecule,  $\text{NH}_3$ , are in the range of a few times  $10^4$  to  $10^8 \text{ cm}^{-3}$  (cf. Garay & Lizano 1999). The expected FUV field at the surface of UCH II regions due to the embedded O4 to B0 type stars ranges from  $10^4$  to greater than  $10^7 G_0$  (Wood & Churchwell 1989b). Thus we estimate the CRL intensities for molecular cloud densities ranging from  $10^4$  to  $10^8 \text{ cm}^{-3}$  and  $G$  ranging from  $10^4$  to  $10^7 G_0$ . For the parameters of the UCH II region, the observed values of W48A are used (see Section 4).

The CRL emission is calculated for a set of 63 PDR models for a grid in the  $G - n$  plane. The results are further re-gridded into a fine grid. In Fig 4 we plot the variation of the ratio of line intensities between the transitions  $\text{C}92\alpha$  (8.3135 GHz),  $\text{C}76\alpha$  (14.6973 GHz) and  $\text{C}53\alpha$  (45.4764 GHz), in the  $G - n$  plane. The parameters which have been assumed for the FWHM of the telescope beam and the distance to the cloud do not affect the line ratios. The contours of the line ratio,  $\text{C}92\alpha/\text{C}76\alpha$  clearly distinguish the density of the PDR but mostly independent of the FUV field. The line ratio,  $\text{C}76\alpha/\text{C}53\alpha$  shows a similar dependence but two densities are possible for a given observed line ratio. These figures show that ob-

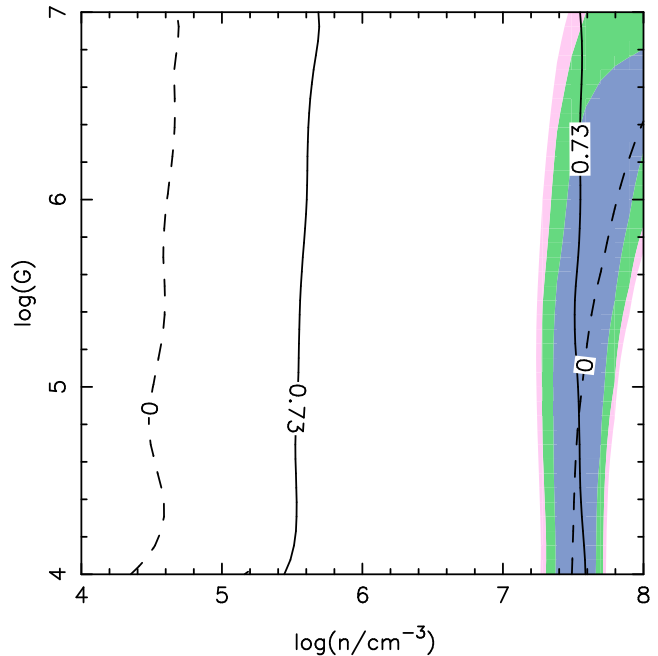


**Figure 5.** The contours of the observed line ratios  $\text{C}76\alpha/\text{C}53\alpha$  (solid) and  $\text{C}92\alpha/\text{C}76\alpha$  (dashed) towards W48A are plotted in the  $G - n$  plane. The intersection of the contours of the observed CRL ratios gives a PDR density of about  $4 \times 10^7 \text{ cm}^{-3}$  and an FUV field of about  $7 \times 10^4 G_0$ . The chi-square contours corresponding to 1 (cyan), 2 (green) and 3 (magenta)  $\sigma$  confidence regions of the fit are plotted with decreasing levels of grey shaded regions.

servations at a suitable set of frequencies will be able to constrain the density of the PDR.

## 4 PDR SURROUNDING THE UCHII REGION W48A

The UCH II region W48A is located in the high mass star-forming region G35.20–1.74 at a distance of about 3.27 kpc (Wood & Churchwell 1989a; Zhang et al. 2009). W48A has been observed both in continuum and spectral line with the VLA at many frequencies by Roshi et al. (2005b). The continuum emission towards W48A can be well fit by a constant density spherical UCH II region model. Based on this fit the estimated parameters of W48A are: the radius of the UCH II region,  $R_{\text{HII}}$  is  $0.059 \text{ pc}$ ; the EM of the background continuum is  $6.4 \times 10^7 \text{ pc cm}^{-6}$  and the temperature of the ionised gas is  $0.99 \times 10^4 \text{ K}$  (Roshi et al. 2005b). CRL emission is detected at 14 ( $\text{C}76\alpha$ ) and 45 GHz ( $\text{C}53\alpha$ ) and upper limits have been provided at 8 ( $\text{C}92\alpha$ ) and 4 GHz ( $\text{C}110\alpha$ ,  $\text{C}111\alpha$ ). At the distance of 3.27 kpc, the UCH II region subtends an angle of  $3''.7$ , which is used to convert the model line temperature to line flux density. For further details on the observations see Roshi et al. (2005b).

The observed value of  $\text{C}76\alpha/\text{C}53\alpha$  is  $0.73 \pm 0.28$  and that of  $\text{C}92\alpha/\text{C}76\alpha$  is  $< 0.3$  (after correcting for different beam sizes at different frequencies). Since  $\text{C}92\alpha$  line flux density is an upper limit, it may also represent an undetected absorption line. Modelling also shows that the  $\text{C}92\alpha$  transition can be in emission or in absorption depending on the PDR density and background FUV field (see Section 3.3). Therefore the ratio  $\text{C}92\alpha/\text{C}76\alpha$  is used as  $0.0 \pm 0.3$  to represent both positive and negative upper limits. The CRL line ratio contours using the model results are plotted in Fig 5 for those values observed towards W48A. The chi-square contours

corresponding to 1(cyan), 2(green) and 3(magenta)  $\sigma$  confidence regions of the fit are plotted with decreasing levels of grey shaded regions. The intersection of the contours of the observed CRL ratios gives a PDR density of about  $4 \times 10^7 \text{ cm}^{-3}$  and an FUV field of about  $7 \times 10^4 G_0$ . The  $1\sigma$  confidence region, however, suggests that the allowed density and G values are larger due to large errors in the line ratios. Sensitive CRL observations are needed to further constrain the model parameters.

The FUV field incident on the PDR, estimated from the parameters of the stellar type (O8 – O7.5) obtained by Roshi et al. (2005b), is  $\lesssim 10^6 G_0$  without considering any dust extinction for FUV photons. This value for G can be used to further constrain the of PDR density to a range between  $2.5 - 7 \times 10^7 \text{ cm}^{-3}$ . The range of PDR densities obtained here is about 30% smaller than the range obtained using a homogeneous slab model (Roshi et al. 2005b).

## 5 CONCLUSIONS

We modelled the CRL emission from PDR layers surrounding an UCH II region. The depth dependence of temperature, ionised carbon and electron densities obtained from PDR models have been incorporated into this model. The non-LTE population of the carbon levels is calculated using these temperatures and densities. The CRL emission is presented over a range of PDR parameters. The results are shown in  $G - n$  plane, where  $G$  ranges from  $10^4$  to  $10^7 G_0$  and the density ranges from  $10^4$  to  $10^8 \text{ cm}^{-3}$ . Modelling the observed CRL emission towards W48A yields a density for the ambient medium of about  $4 \times 10^7 \text{ cm}^{-3}$ .

## ACKNOWLEDGEMENTS

We are grateful to the anonymous referee for the critical comments and suggestions. SJ thanks the support offered by the Raman Research Institute for a short visit. We thank J. Le Bourlot for providing us the PDR code. This work was partially supported by PROMEP/103-5/07/2462 and Conacyt CB-2009-01/130523 grants.

## REFERENCES

- Arthur S. J., Kurtz S. E., Franco J., Albarrán M. Y., 2004, *ApJ*, 608, 282
- Bertoldi F., Draine B. T., 1996, *ApJ*, 458, 222
- Churchwell E., 1993, in *ASP Conf. Ser. 35: Massive Stars: Their Lives in the Interstellar Medium*, p. 35
- , 2002, *ARA&A*, 40, 27
- Churchwell E., Walmsley C. M., Cesaroni R., 1990, *A&AS*, 83, 119
- de Pree C. G., Rodriguez L. F., Goss W. M., 1995, *Revista Mexicana de Astronomia y Astrofisica*, 31, 39
- Dupree A. K., Goldberg L., 1970, *ARA&A*, 8, 231
- Franco J., García-Segura G., Kurtz S. E., Arthur S. J., 2007, *ApJ*, 660, 1296
- Franco J., Kurtz S. E., García-Segura G., Hofner P., 2000, *Ap&SS*, 272, 169
- Franco J., Tenorio-Tagle G., Bodenheimer P., 1990, *ApJ*, 349, 126
- Garay G., Lizano S., 1999, *PASP*, 111, 1049
- Goldshmidt O., Sternberg A., 1995, *ApJ*, 439, 256
- Gomez Y., Lebron M., Rodriguez L. F., Garay G., Lizano S., Escalante V., Canto J., 1998, *ApJ*, 503, 297
- Habing H. J., 1968, *Bull. Astron. Inst. Netherlands*, 19, 421
- Hollenbach D., Natta A., 1995, *ApJ*, 455, 133
- Hollenbach D. J., Tielens A. G. G. M., 1997, *ARA&A*, 35, 179
- Keto E., Zhang Q., Kurtz S., 2008, *ApJ*, 672, 423
- Kim K., Koo B., 2003, *ApJ*, 596, 362
- Kurtz S., Churchwell E., Wood D. O. S., 1994, *ApJS*, 91, 659
- Kurtz S., Franco J., García-Barreto J. A., Hofner P., García-Segura G., de La Fuente E., Esquivel A., 2001, in *Revista Mexicana de Astronomia y Astrofisica Conference Series*, pp. 45–48
- Le Bourlot J., Pineau Des Forets G., Roueff E., Flower D. R., 1993, *A&A*, 267, 233
- Le Petit F., Nehmé C., Le Bourlot J., Roueff E., 2006, *ApJS*, 164, 506
- Mezger P. G., Henderson A. P., 1967, *ApJ*, 147, 471
- Natta A., Walmsley C. M., Tielens A. G. G. M., 1994, *ApJ*, 428, 209
- Payne H. E., Anantharamaiah K. R., Erickson W. C., 1994, *ApJ*, 430, 690
- Peters T., Mac Low M.-M., Banerjee R., Klessen R. S., Dullemond C. P., 2010, *ApJ*, 719, 831
- Phillips J. P., 2007, *MNRAS*, 380, 369
- Roelfsema P. R., Goss W. M., 1992, *A&A Rev.*, 4, 161
- Roger R. S., Dewdney P. E., 1992, *ApJ*, 385, 536
- Roshi D. A., Balser D. S., Bania T. M., Goss W. M., De Pree C. G., 2005a, *ApJ*, 625, 181
- Roshi D. A., Goss W. M., Anantharamaiah K. R., Jeyakumar S., 2005b, *ApJ*, 626, 253
- Roshi D. A., Kantharia N. G., Anantharamaiah K. R., 2002, *A&A*, 391, 1097
- Salem M., Brocklehurst M., 1979, *ApJS*, 39, 633
- Sewilo M., Churchwell E., Kurtz S., Goss W. M., Hofner P., 2008, *ApJ*, 681, 350
- Shaver P. A., 1975, *Pramana*, 5, 1
- Tielens A. G. G. M., Hollenbach D., 1985, *ApJ*, 291, 722
- Walmsley C. M., Watson W. D., 1982, *ApJ*, 260, 317
- Wood D. O. S., Churchwell E., 1989a, *ApJ*, 340, 265
- , 1989b, *ApJS*, 69, 831
- Wyrowski F., Schilke P., Hofner P., Walmsley C. M., 1997, *ApJ*, 487, L171
- Zhang B., Zheng X. W., Reid M. J., Menten K. M., Xu Y., Moscadelli L., Brunthaler A., 2009, *ApJ*, 693, 419

This paper has been typeset from a  $\text{\TeX}/\text{\LaTeX}$  file prepared by the author.